

---

# High-Resolution Imaging with $^{99m}\text{Tc}$ -Glucarate for Assessing Myocardial Injury in Rat Heart Models Exposed to Different Durations of Ischemia with Reperfusion

Zhonglin Liu, MD<sup>1</sup>; Harrison H. Barrett, PhD<sup>1</sup>; Gail D. Stevenson, DVM<sup>1</sup>; George A. Kastis, PhD<sup>1</sup>; Michael Bettan, MS<sup>1</sup>; Lars R. Furenid, PhD<sup>1</sup>; Donald W. Wilson, PhD<sup>1</sup>; and Koon Yan Pak, PhD<sup>2</sup>

<sup>1</sup>Department of Radiology, The University of Arizona, Tucson, Arizona; and <sup>2</sup>Molecular Targeting Technologies Inc., West Chester, Pennsylvania

---

$^{99m}\text{Tc}$ -Glucarate ( $^{99m}\text{Tc}$ -GLA) is a novel infarct-avid imaging agent. The aim of this study was to evaluate the role of  $^{99m}\text{Tc}$ -GLA for assessing the severity of myocardial ischemia-reperfusion injury in rat heart models exposed to varied durations of left coronary artery (LCA) occlusion with reperfusion using a high-resolution SPECT system, FASTSPECT. We also wanted to clarify whether a rapid sequence of 3-dimensional imaging with FASTSPECT can quantify uptake and washout kinetics of cardiovascular imaging agents in small-animal heart models. **Methods:** The ischemia-reperfused rat heart models were created by ligating the LCA for 30 min (IR30,  $n = 12$ ) or 90 min (IR90,  $n = 6$ ) (IR = ischemia-reperfusion) and releasing the ligature for 30 min. Dynamic images were acquired over a 2-h period after  $^{99m}\text{Tc}$ -GLA was intravenously injected. The ischemic area at risk (IAR) was determined by Evans blue staining. Necrosis was assessed with triphenyltetrazolium chloride (TTC) staining and a transmission electron microscope (TEM). **Results:** The infarct size of the left ventricle (% IAR) on TTC staining was smaller in IR30 ( $49.2 \pm 4.3$ ) than in IR90 ( $73.4 \pm 4.7$ ,  $P < 0.05$ ), which exhibited evidence of more severe irreversible injury than the IR30 heart on TEM. FASTSPECT images demonstrated hot spot accumulations of  $^{99m}\text{Tc}$ -GLA in all hearts. The washout of  $^{99m}\text{Tc}$ -GLA from the ischemic-reperfused area in IR90 was significantly slower than that in IR30. The ratio of the hot spot to normal myocardial activity was  $4.1 \pm 0.3$  in IR30 and  $7.1 \pm 1.1$  in IR90 ( $P < 0.05$ ). The hot spot size (% IAR) ( $58.4 \pm 2.7$  in IR30 vs.  $75.9 \pm 2.7$  in IR90,  $P < 0.05$ ) related significantly to the infarct size. **Conclusion:** The severity of myocardial injury induced by ischemia-reperfusion can be assessed by FASTSPECT imaging with  $^{99m}\text{Tc}$ -GLA. The results suggest that  $^{99m}\text{Tc}$ -GLA will be clinically useful in detecting and quantifying acute necrotic myocardium. The FASTSPECT imaging with the rat heart models provides a solution-specific approach with high-resolution and fast dynamic acquisition for kinetic studies of new myocardial imaging agents.

**Key Words:**  $^{99m}\text{Tc}$ -glucarate; ischemia-reperfusion injury; rat heart; high-resolution SPECT

**J Nucl Med 2004; 45:1251-1259**

---

**I**n mammals, D-glucaric acid (glucarate, GLA) is a 6-carbon dicarboxylic acid sugar and a natural catabolite of glucuronic acid metabolism (1,2). All mammals excrete glucaric acid as a physiologic end product. GLA can be readily radiolabeled with sodium pertechnetate, resulting in  $^{99m}\text{Tc}$ -GLA. Experimental studies have shown the favorable targeting potential of  $^{99m}\text{Tc}$ -GLA of severe ischemia or early necrosis of the heart and brain (1-4). In acutely injured cells, it is believed that  $^{99m}\text{Tc}$ -GLA is associated with disruption of the myocyte and nuclear membranes, allowing free intracellular diffusion and electrochemical binding of the negatively charged GLA complex to positively charged histones. This intracellular distribution is driven by the avidity of GLA to the nuclear protein and cytoplasmic proteins with a positive charge. In rat models with isoproterenol-induced myocardial infarction,  $^{99m}\text{Tc}$ -GLA uptake in the infarcted hearts was found 6 times more than in normal rats (5).  $^{99m}\text{Tc}$ -GLA has been proposed as a specific oncotic marker in the very early stages of myocyte injury but not as an apoptotic marker (6). As an infarct-avid agent, the early distribution in necrotic myocardium and rapid blood-pool clearance of  $^{99m}\text{Tc}$ -GLA suggest important diagnostic potential in early detection of acute myocardial infarction and identification of successful acute revascularization therapy.

To date, few studies have been done regarding  $^{99m}\text{Tc}$ -GLA imaging in ischemia-reperfused myocardium with varied severity of injury. This study was conducted to determine whether the amount of myocardial damage in the hearts with ischemia-reperfusion is associated with myocardial accumulation levels of  $^{99m}\text{Tc}$ -GLA. It is not known whether this association is reflected in the degree of myo-

---

Received Oct. 30, 2003; revision accepted Jan. 16, 2004.  
For correspondence or reprints contact: Zhonglin Liu, MD, Department of Radiology, The University of Arizona, P.O. Box 245067, Tucson, AZ 85724-5067.  
E-mail: zliu@radiology.arizona.edu

cardial injury in the ischemic–reperfused hearts. First, severity of injury can be estimated by the size of infarct or amount of irreversible myocytic necrosis. In clinical patients, infarct size can be determined with several noninvasive techniques, which has significance for general prognosis in patients after acute heart attack. Since  $^{99m}\text{Tc}$ -GLA is accumulated by acute necrotic myocardium only, we speculated that  $^{99m}\text{Tc}$ -GLA hot spot imaging might be ideal for noninvasively determining infarct size with a SPECT camera. Using well-defined in vivo rat heart models, we acquired  $^{99m}\text{Tc}$ -GLA images with a novel high-resolution stationary SPECT system called FASTSPECT. Ischemia–reperfusion injury was analyzed by triphenyltetrazolium chloride (TTC) staining and electron microscope examination. We quantified and compared the infarct size shown by  $^{99m}\text{Tc}$ -GLA imaging with the TTC staining analysis. Second, since the uptake and washout kinetics of viability-dependent imaging agents are altered by the extent and severity of cellular and extracellular structural changes of ischemic–reperfused myocardium, the present study was undertaken to determine the in vivo kinetic properties of  $^{99m}\text{Tc}$ -GLA for assessing the severity of myocardial ischemia–reperfusion injury in rat heart models exposed to different durations of left coronary artery (LCA) occlusion with reperfusion. Using FASTSPECT, dynamic tomographic images were obtained in the beating rat hearts with no motion of detectors or imaging aperture. We wanted to clarify whether a rapid sequence of 3-dimensional (3D) imaging with FASTSPECT can make it possible to visualize the heart with ischemia–reperfusion injury and investigate the kinetics of cardiovascular imaging agents in small-animal in vivo models.

## MATERIALS AND METHODS

### Ischemic–Reperfused Rat Heart Model Preparation

Male Sprague–Dawley rats (weight, 250–300 g) were anesthetized with 1.0%–1.5% isoflurane. The model of myocardial ischemia–reperfusion was developed using the technique described previously (7–9). The rat was prepared by first removing the fur from the chest and neck region with electric clippers. The jugular vein was catheterized through a surgical procedure. An incision was made over the jugular furrow, and blunt and sharp dissection was used to isolate the jugular vein. A PE-10 catheter was advanced through a nick made by micro scissors and then secured by ligatures. After tracheotomy, the rats were ventilated using a volume-controlled Inspira Advanced Safety Ventilator (Harvard Apparatus, Inc.) with a mixture of oxygen and room air. Using each animal's weight, the tidal volume (1.2 mL/100 g) and respiration rate (65–70 breaths/min) were automatically calculated in Safe Range settings (Harvard Apparatus). With a left intercostal thoracotomy incision, the chest was opened at the fourth or fifth intercostal space. The pericardium was opened and the heart was exposed. A small, curved, tapered needle threaded 5-0 silk through the tissue between the pulmonary cone and the left auricular appendage. A ligature was placed around the LCA with a small amount of myocardium. The ligature was pulled tight by passing the suture through a polyethylene tubing and clamping it for

coronary occlusion. After the LCA was occluded for 30 or 90 min, 30 min of reperfusion was achieved by releasing the ligature. Hydrochloride lidocaine (5%) was administered via intravenous injection and cardiac surface drop when ventricular fibrillation was induced by LCA occlusion or reflow. During the period of surgery and ischemia–reperfusion treatment, the body temperature of the animal was maintained with a heating pad. The chest of the rat was closed before the animal was imaged with FASTSPECT.

### Experimental Groups and Study Protocols

Eighteen rats were divided into 2 groups to receive regional myocardial ischemia–reperfusion treatments. Group 1 animals (IR30,  $n = 12$  [IR = ischemia–reperfusion]) were treated by ligating the LCA for 30 min and releasing the ligature for 30 min. The LCA in group 2 animals (IR90,  $n = 6$ ) was ligated for 90 min and then released for 30 min. The experimental protocols are showed in Figure 1.

### Radiopharmaceutical Preparation

GLA kits were provided by Molecular Targeting Technologies Inc. The reagent in the vial was a sterile, nonpyrogenic, lyophilized composition of potassium chloride, GLA, sodium bicarbonate, and hydrochloric acid. A vial of GLA was reconstituted by the addition of 1 mL of  $^{99m}\text{Tc}$  as sodium pertechnetate (no < 2.59 GBq [no < 70 mCi]) in accordance with the manufacturer's instructions. The solution in the vial was allowed to stand at room temperature for 15 min.  $^{99m}\text{Tc}$ -GLA radiochemical purity (RCP) was verified by thin-layer liquid chromatography using Gelman instant thin-layer silica gel (ITLC-SG) strips developed in saline and acetone. In the ITLC-SG strip developed by saline,  $^{99m}\text{Tc}$ -colloid remained at the origin while  $^{99m}\text{Tc}$ -GLA and  $^{99m}\text{Tc}$ -pertechnetate migrated near the solvent front. In the strip developed by acetone,  $^{99m}\text{Tc}$ -GLA and  $^{99m}\text{Tc}$ -colloid remained at the origin while  $^{99m}\text{Tc}$ -pertechnetate moved near the solvent front. The RCP of  $^{99m}\text{Tc}$ -GLA exceeded 95% for all experimental injections.  $^{99m}\text{Tc}$ -GLA was used within 3 h after preparation.

### FASTSPECT System

The high-resolution stationary SPECT system, FASTSPECT, was built in the Department of Radiology Research Laboratory at The University of Arizona (9–11). In this system, 24 small mod-

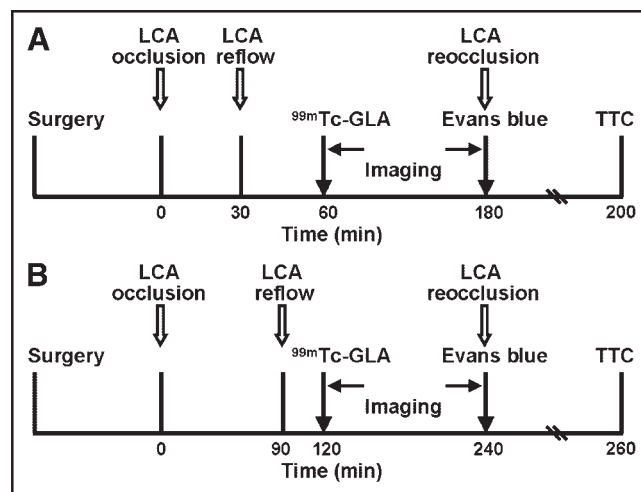


**FIGURE 1.** Experimental protocols in group 1 (A) and group 2 (B).

ular  $\gamma$ -cameras are arranged in 2 circular arrays with a cylindrical aperture. Each modular camera possesses a  $10 \times 10$  cm Rexon NaI(Tl) scintillation crystal (Rexon Components, Inc.), an optical light guide, 4 square ( $5 \times 5$  cm) Hamamatsu Photonics photomultiplier tubes, and driver/amplifier electronics. Twenty-four 1-mm-diameter pinholes were drilled in the aperture such that a point source in the center of the field of view (FOV) is simultaneously projected to the center of each camera. The dead space between adjacent cameras at the detector surface is  $<7\%$  of the total area. The total magnification is 3.5 in a  $3.0 \times 3.2 \times 3.2$  cm FOV. The spatial resolution of the system is about 1.0 mm with a sensitivity of 0.359 cps/kBq (13.3 cps/ $\mu$ Ci) in air.

### FASTSPECT Imaging

The rat was placed inside the aperture using a 6-cm-diameter cylindrical cardboard holder mounted on a translation stage. The animal was positioned so that the heart localized in the center of the FOV. Thirty minutes after LCA reflow,  $^{99m}\text{Tc}$ -GLA (148–296 MBq [4–8 mCi]) was injected as a bolus via the jugular vein catheter, followed by a 0.2-mL saline flush. Dynamic images were acquired every 1 min for 10 min beginning immediately on injection, followed by 5-min acquisitions at 15, 20, and 30 min. Then 5-min images were obtained every 15 min from 30 to 120 min after injection. A total of 24 projections were obtained, one from each camera. Each projection image was formed using a 24-bit word as an entry to a precomputed look-up table scheme. In this scheme, each scintillation event within the NaI crystal of the camera was registered as the digitized outputs from the camera's 4 photomultiplier tubes. To estimate energy and interaction position, the 4 outputs were then compared with the 20-bit look-up table. This table was precalculated using a calibration procedure that involved moving a collimated source across the camera face (12).

### Image Processing

The maximum-likelihood expectation-maximization reconstruction algorithm was applied to generate 3D images. All images were reconstructed using 100 iterations. Using SlicerDicer software (PIXOTEC LLC), 3D images were computed to provide images in a  $33 \times 49 \times 49$  voxels format, reoriented manually regarding the cardiac axis. Then serial tomographic short-axis, vertical, and horizontal long-axis slices of the heart with 1-pixel thickness (1.0 mm) were generated.

A region of interest (ROI) was established over a hot spot with the highest activity of  $^{99m}\text{Tc}$ -GLA (counts/pixel) selected from a short-axis slice of the 120-min image. The ROI was applied to all images from 1 to 120 min after injection. After correction for background and  $^{99m}\text{Tc}$  decay, the radioactivity (counts/pixel/min) in the hot spot was projected onto the dynamic images to determine the time-activity curve. Using an ROI selected from the non-LCA region (left ventricular septum), the normal myocardial time-activity curve was generated and compared with the curve of the infarct zone. Hot spots on all short-axis slices of 120-min image were quantified with ROI analysis to calculate the ratios of necrotic zone activities to normal myocardial activities and averaged over the whole heart to produce a mean ratio.

### Measurement of Myocardial Risk and Infarct

After imaging acquisition was completed, the animal was moved out of the aperture. The chest of the rat was reopened and the LCA was reoccluded using the same ligature. To determine the myocardial ischemic area at risk (IAR), 1.0 mL Evans blue (20%) in phosphate-buffered saline (PBS) was injected through the fem-

oral vein, allowing dye to stain the nonischemic portion of the heart. The risk zone was identified as that region lacking blue staining. An overdose injection of pentobarbital was followed immediately to kill the animal. The entire heart was expeditiously excised, weighed, and rinsed of excess dye with cold saline.  $^{99m}\text{Tc}$  activity in the heart was measured in a CRC-4 radioisotope dose calibrator (Capintec). The great vessels, atria, and right ventricle of the heart were removed. The left ventricle was sectioned into 4 transverse slices in a plane parallel to the atrioventricular groove. Both sides of each tissue slice were photographed immediately using a D-500L digital camera (Olympus Optical Co.).

TTC staining was used to identify the area with infarct. The tissue slices were incubated in 1% TTC PBS solution (pH = 7.4) at  $37^\circ\text{C}$  for 20 min and subsequently fixed in 10% PBS-buffered formalin overnight at  $2^\circ\text{C}$ – $8^\circ\text{C}$ . The viable myocardium stained by TTC was dark red. Both sides of each TTC-stained tissue slice were photographed again with the digital camera.

The IAR (unstained by Evans blue dye) and the TTC-negative area (white or pale, necrotic myocardium) on the digital photographs were outlined and quantified using the SigmaScan software (SPSS Science) in trace-measurement mode. Infarct size was expressed both as a percentage of total LV mass (% LV) and as a percentage of the IAR (% IAR).

### Determination of Infarct on FASTSPECT Imaging

The hot spot size of  $^{99m}\text{Tc}$ -GLA on the 120-min image was determined on short-axis slices using the trace-measurement mode of SigmaScan software as described. The left ventricular wall was outlined using the 1-min cardiac blood-pool image as a contrast. The size of hot spots on short-axis slices were averaged as a percentage of the entire left ventricle and then normalized to the percentage of the IAR (% IAR).

### Assessment of Ultrastructural Injury

An additional 4 rats were subjected to the experimental protocol without radiotracer administration. Two rat hearts were treated as the IR30 protocol in group 1; others were treated as the IR90 protocol in group 2. After a 30-min reperfusion, 0.5 mL saline was intravenously injected to match the injected volume of  $^{99m}\text{Tc}$ -GLA and saline in group 1 and group 2. The anesthetized rats were kept alive under the same experimental conditions as described for 2 h and then killed at the end of the experiment. Two small blocks of left ventricular tissue were selected from the LCA ischemic-reperfused central area and nonischemic area (septum) of each heart, respectively. The tissue blocks were immersed in a phosphate-buffered 3% glutaraldehyde solution (pH 7.4) for 3 h at  $4^\circ\text{C}$ . Then the samples were transferred and postfixated in 1% osmium tetroxide, dehydrated in a graded series of ethanol, and embedded in epoxy resin. Ultrathin sections were stained with uranyl acetate and lead hydroxide and examined with a transmission electron microscope ([TEM] Phillips CM12).

### Data Analysis

All results are expressed as mean  $\pm$  SEM. Comparisons between groups were performed with 1-way ANOVA. Comparisons between 2 variables within a group were made using a paired *t* test. Probability values  $< 0.05$  were considered significant. The correlation between myocardial  $^{99m}\text{Tc}$ -GLA hot spots and myocardial infarct size as measured by TTC stain was assessed by linear regression analysis.

Hot spot and normal zone activities were normalized to peak activities at 2 min for each experiment and averaged for the group

to produce mean myocardial time-activity washout curves. The kinetic washout curves of  $^{99m}\text{Tc}$ -GLA were fit with nonlinear regression procedures using TableCurve 2-dimensional software (Systat Software, Inc.).

### Ethics

All experiments were performed in accordance with the animal research guidelines of the National Research Council (13) and were approved by the Institutional Animal Care and Use Committee at The University of Arizona.

## RESULTS

### FASTSPECT Images of Myocardium with Ischemia-Reperfusion

A representative reconstructed 3D display of 120-min FASTSPECT images of a rat heart subjected to the IR90 protocol is shown in Figure 2A. The wall of the left ventricle was partly visualized in the stenosis zone of LCA-supplied area. Selected tomographic short-axis, horizontal,

and vertical long-axis slices of the heart are showed in Figures 2A, 2B, and 2C, respectively, which exhibit a hot spot (increased  $^{99m}\text{Tc}$ -GLA uptake) localized on the anterior wall, lateral wall, and apex of the left ventricle. Identical hot spots were detected in all rat hearts of group 1 and group 2 with ischemia-reperfusion imaged with  $^{99m}\text{Tc}$ -GLA. A good infarct definition with the regional hot spot could be achieved 10 min after intravenous administration. The infarct remained well defined for at least 120 min after injection. Figure 3 demonstrates representative  $^{99m}\text{Tc}$ -GLA in vivo FASTSPECT dynamic images in an IR30 heart.

### Quantitative Analysis of $^{99m}\text{Tc}$ -GLA Imaging

Myocardial  $^{99m}\text{Tc}$ -GLA activities were quantified with the computerized ROI analysis of FASTSPECT images that were background-subtracted and decay-corrected. Figure 4A shows normalized myocardial time-activity washout curves.  $^{99m}\text{Tc}$ -GLA exhibited biphasic washout from the

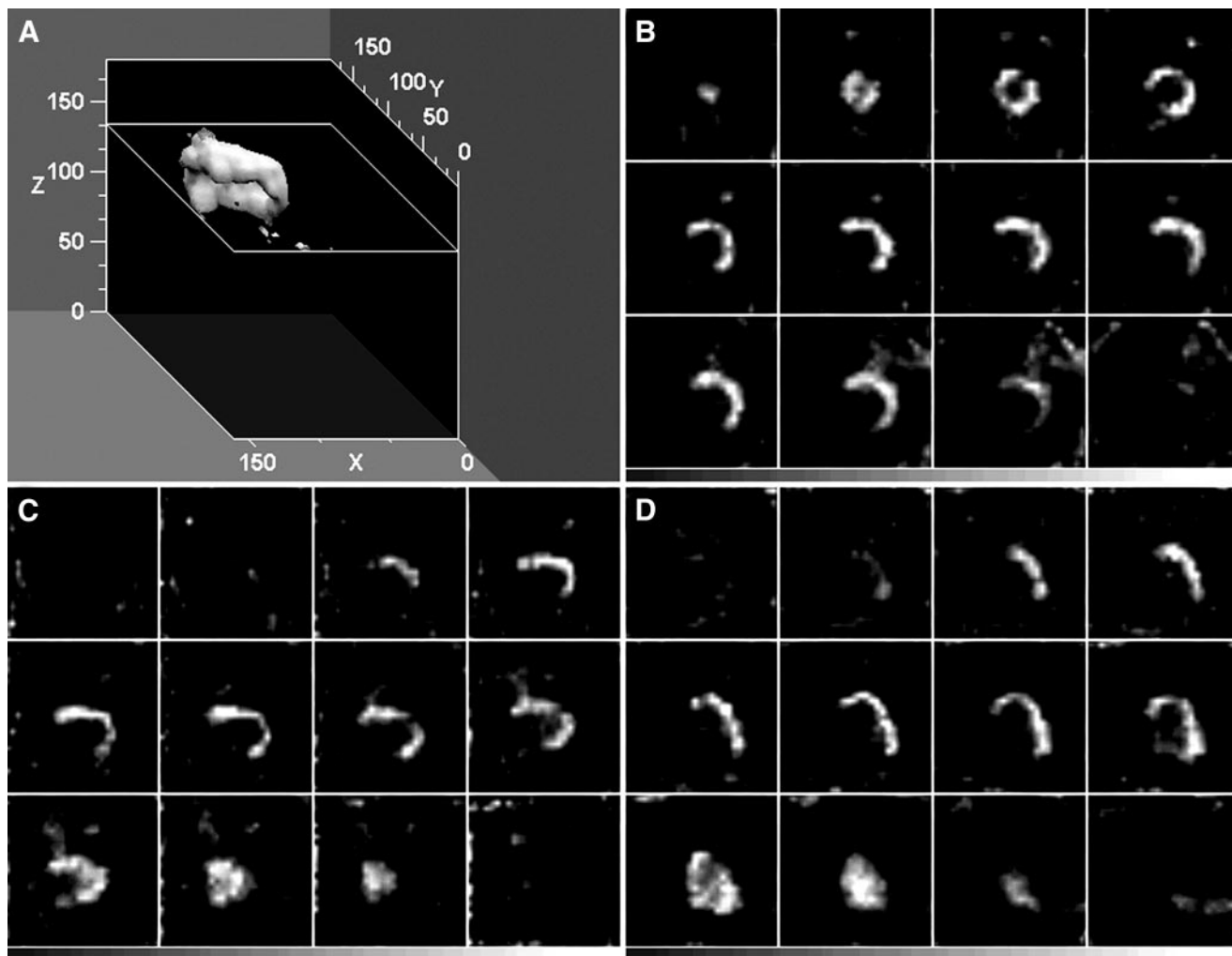


**FIGURE 2.** (A) Three-dimensional representation of reconstructed FASTSPECT dataset of left ventricle in rat treated with IR90 protocol 120 min after injection with  $^{99m}\text{Tc}$ -GLA. Wall of left ventricle was partly visualized in stenotic zone of LCA-supplied area, including lateral wall, part of anterior wall, and apex. (B–D) Selected tomographic short-axis, vertical, and horizontal long-axis slices, respectively, with  $^{99m}\text{Tc}$ -GLA hot spot accumulations on lateral wall, anterior wall, and apex.

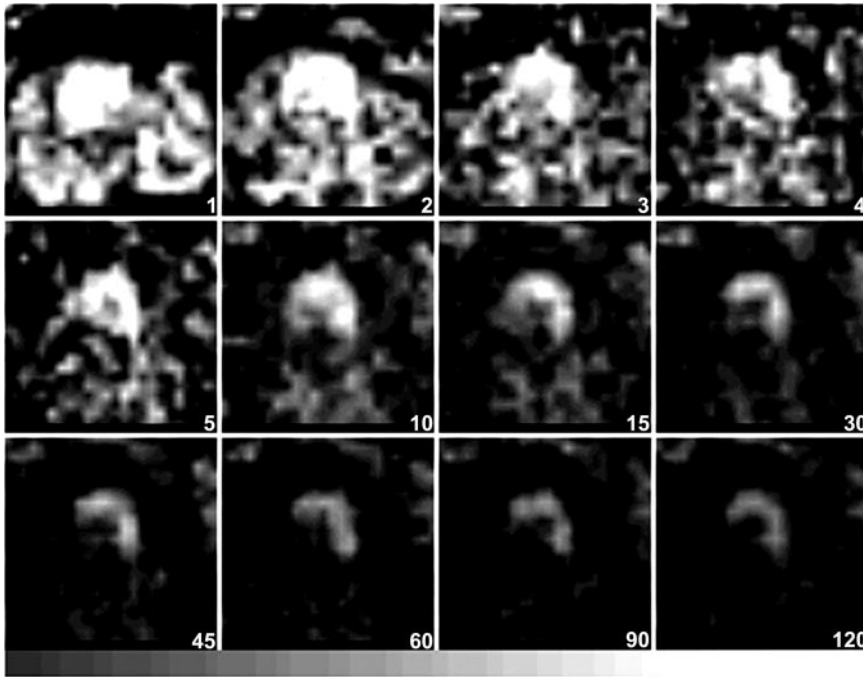


**FIGURE 3.** Dynamic tomographic images (short axis) of  $^{99m}\text{Tc}$ -GLA in heart subjected to 30-min ischemia followed by 30-min reperfusion from 1 to 120 min after injection. Blood pool was shown in 1-min image; an unequivocal hot spot was found on anterior and lateral wall of left ventricle from 10 to 120 min.

LCA hot spot and normal myocardial zone. The kinetic washout curves were plotted from 2 to 120 min with a significant difference observed at each point in time from 10 to 120 min between the LCA hot spot and normal zone in group 1 and group 2. Beginning at 75 min, the normalized hot spot activity in group 2 was significantly higher than that in group 1. Total 2-h fractional washout from the hot spot was significantly lower than that of the normal zone. As a result, the fractional retention (% peak) was significantly higher in the hot spot than that in the normal zone ( $31.0 \pm 1.3$  vs.  $7.5 \pm 1.0$  in IR30,  $P < 0.05$ ;  $42.1 \pm 4.0$  vs.  $6.4 \pm 0.9$  in IR90,  $P < 0.05$ ) by the end of experiment. The hot spot of group 2 exhibited significantly higher  $^{99m}\text{Tc}$ -GLA retention than that of group 1 ( $P < 0.05$ ). By fitting each individual curve using the TableCurve calculation, biexponential equations were found to provide the best fits to the curves. The early phase showed fast washout and the late phase showed slow washout. The best fit equation was:  $y = a \cdot \exp(-bx) + c \cdot \exp(-dx)$ . There was no significant difference in the half-time value ( $t_{1/2}$ ) for the early phase between the hot spot and normal zone (IR30:  $2.4 \pm 0.4$  vs.  $1.6 \pm 0.4$ ,  $P > 0.05$ ; IR90:  $3.8 \pm 1.1$  vs.  $2.0 \pm 0.2$ ,  $P > 0.05$ ). However, there was a significant difference ( $P < 0.05$ ) for the  $t_{1/2}$  in the late phase (IR30:  $216.3 \pm 23.8$  vs.  $66.6 \pm 5.5$ ,  $P < 0.05$ ; IR90:  $511.5 \pm 74.2$  vs.  $49.1 \pm 2.9$ ,  $P < 0.05$ ).

Figure 4B shows that the ratios of the hot spots to normal myocardial activities increased progressively after  $^{99m}\text{Tc}$ -GLA administration in the IR30 and IR90 hearts. Beginning at 45 min, the ratio in group 2 was significantly higher than that in group 1. The final ratio was  $4.91 \pm 0.71$  in group 1 and  $9.53 \pm 1.76$  in group 2 ( $P < 0.05$ ). The ratio in group 1 with the IR30 protocol was 1.94-fold lower than that in group 2 with the IR90 protocol. Two hours after injection,

the averaged ratio of the whole-heart hot spot activity to normal myocardial activity was  $4.1 \pm 0.3$  in group 1 and  $7.1 \pm 1.1$  in group 2 ( $P < 0.05$ ).

#### Myocardial IAR and Infarct Size

The measurements of myocardial ischemic IAR and infarct are shown in Table 1. The difference of myocardial ischemic IARs as shown by lack of Evans blue between the hearts subjected to 30- and 90-min LCA occlusion was not significant. The  $^{99m}\text{Tc}$ -GLA hot spots on FASTSPECT images were consistent with the unstained areas on TTC staining (Fig. 5A and 5B). The percent infarct size of left ventricles measured by TTC staining in group 1 was significantly smaller than that of group 2. Normalized by the ischemic IAR, the infarct size (% IAR) in group 1 was still significantly smaller than that of group 2. The quantified hot spots with  $^{99m}\text{Tc}$ -GLA on FASTSPECT imaging represented a good agreement with the infarct measurements on TTC staining. The hearts subjected to 90-min LCA occlusion exhibited significantly larger hot spots compared with the hearts subjected to 30-min LCA occlusion ( $P < 0.05$ ). There was a significant correlation between the infarct measurements (corrected by IAR, % IAR) with TTC staining and  $^{99m}\text{Tc}$ -GLA FASTSPECT imaging in either group 1 ( $r = 0.797$ ,  $P = 0.0019$ ) or group 2 ( $r = 0.956$ ,  $P = 0.0029$ ). Figure 6 illustrates the overall correlation between the measurements in all 18 experimental hearts ( $r = 0.912$ ,  $P < 0.0001$ ).

#### Electron Microscope Analysis

Representative electron photomicrographs made of thin sections of myocardial tissue samples for group 1 and group 2 are shown in Figure 7. There were no significant TEM morphologic differences noted among sections taken from

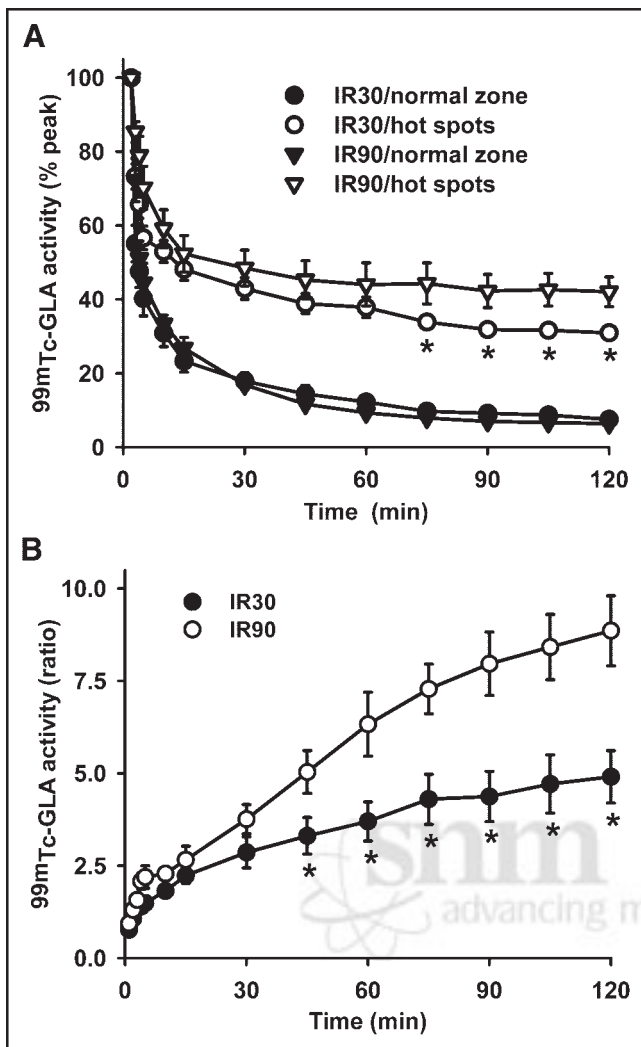


**FIGURE 4.** (A)  $^{99m}\text{Tc}$ -GLA kinetic washout curves from normal and ischemic-reperfused areas in group 1 (IR30) and group 2 (IR90) hearts. Curves were normalized to 100% of initial peak activity. \* $P < 0.05$  compared with IR90. (B) Ratios of hot spots to viable myocardial  $^{99m}\text{Tc}$ -GLA activities over time from hearts of group 1 (IR30) and group 2 (IR90). \* $P < 0.05$  compared with IR90.

the septa of the left ventricles of the hearts subjected to 30- or 90-min LCA occlusion followed by reperfusion. These samples exhibited a normal morphologic appearance. In contrast, hearts subjected to the ischemia-reperfusion treat-

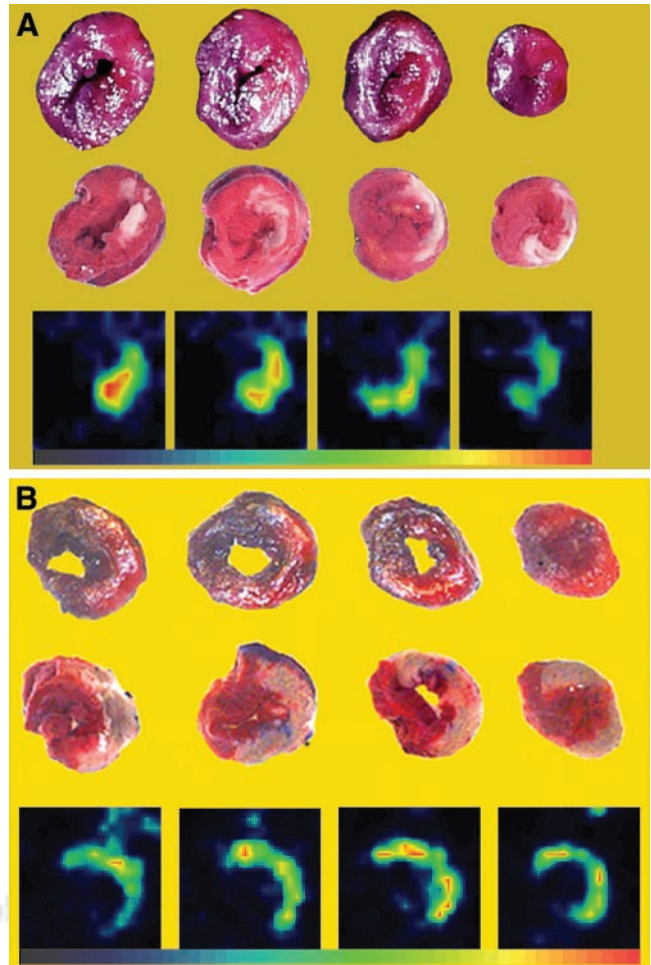


**FIGURE 5.** Hot spots were exhibited on  $^{99m}\text{Tc}$ -GLA images (bottom row) from representative IR 30 heart (A) and IR90 heart (B) subjected to 30- and 90-min ischemia treatments followed by reperfusion, which were consistent with myocardial IARs evaluated by Evans blue (unstained by blue dye) (top row) and infarcts determined by TTC staining (unstained) (middle row). Size of infarct and hot spot was relatively smaller in IR30 heart than that in IR90 heart.

ment showed abnormalities in mitochondrial and myofilament morphology with irreversible myocytic injury indicated by electron-dense inclusions and membrane breaks.

In contrast to the 30-min ischemia heart, the 90-min ischemia heart exhibited evidence of more severe, irrevers-

**TABLE 1**  
Myocardial IAR and Infarct Measurements

Parameter	IAR (% LV)	TTC (% LV)	TTC (% IAR)	GLA (% LV)	GLA (% IAR)
IR30 ( $n = 12$ )	$48.8 \pm 3.2$	$24.5 \pm 3.2$	$49.2 \pm 4.3$	$28.4 \pm 2.1$	$58.4 \pm 2.7$
IR90 ( $n = 6$ )	$55.2 \pm 1.8$	$40.8 \pm 3.6^*$	$73.4 \pm 4.7^*$	$42.0 \pm 2.6^*$	$75.9 \pm 2.7^*$

\* $P < 0.05$  compared with IR30.

% LV = % LV mass.

Data are expressed as mean  $\pm$  SEM.

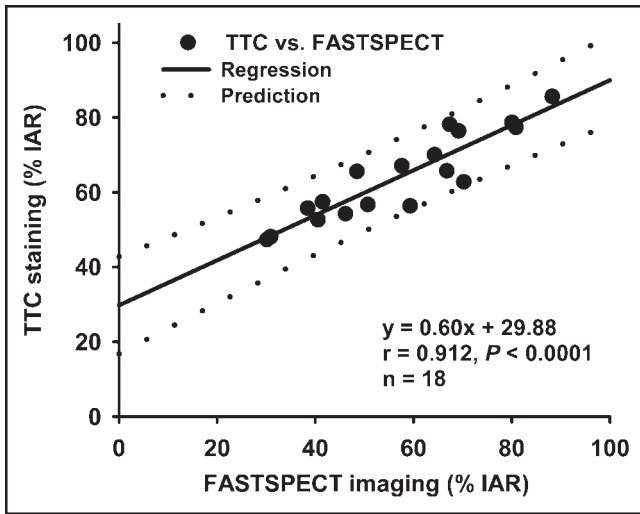


**FIGURE 6.** Scatter plot illustrates relationship between infarct measurements by  $^{99m}\text{Tc}$ -GLA FASTSPECT imaging and TTC staining.

ible injury, including breaks in sarcolemma, abnormal nucleus, hyperplasia of mitochondria, and dense intramitochondrial granules. Matrix dilution, swelling, fenestration, and paucity of cristae with loss of cytosolic glycogen were found in most mitochondria.

## DISCUSSION

In this study, dynamic high-resolution SPECT imaging enabled detection of myocardial hot spots in rat heart models exposed to 30- and 90-min LCA occlusion followed by reperfusion with  $^{99m}\text{Tc}$ -GLA. Ischemic-reperfused treatments in the 2 models produced an average infarct size of

24.5% and 40.8%, respectively, with a significant difference. The difference in severity of ischemia-reperfusion injury between the 2 rat heart models was confirmed by ultrastructural electron microscope examination. Dynamic FASTSPECT  $^{99m}\text{Tc}$ -GLA imaging demonstrated a good infarct definition 10 min after injection. The infarct remained well defined for at least 120 min after injection. The ratio of the hot spot to normal myocardial activity increased progressively after  $^{99m}\text{Tc}$ -GLA administration. Beginning at 45 min after injection, the ratios in hearts subjected to 90-min LCA occlusion and reperfusion were significantly greater than that in hearts subjected to 30-min LCA occlusion. The slower kinetic washout of  $^{99m}\text{Tc}$ -GLA in the IR90 hearts resulted in a significantly higher radioactive retention compared with that of the IR30 hearts. The hot spots of the IR90 hearts with  $^{99m}\text{Tc}$ -GLA on FASTSPECT imaging, which represented a good agreement with the infarct measurements on TTC staining, were significantly larger relative to the IR30 hearts. These results confirm that  $^{99m}\text{Tc}$ -GLA is preferentially retained in acute necrotic myocardium after onset of coronary occlusion. More important, the amount of retention of  $^{99m}\text{Tc}$ -GLA and the size of the hot spot in ischemic-reperfused myocardium are correlated with the severity of myocardial injury.

$^{99m}\text{Tc}$ -GLA has been tested in a variety of animal models to investigate its infarct-avid localizing properties, including ex vivo isolated perfused rat and rabbit hearts and in vivo rabbit, canine, and swine heart models (2,3,14,15). Using a swine model with myocardial ischemia induced by a catheter-mounted stenosis in the left anterior descending coronary artery, Johnson et al. reported positive uptake of  $^{99m}\text{Tc}$ -GLA in the severe ischemic myocardium (15). Of the 15  $^{99m}\text{Tc}$ -GLA scan-positive studies, 8 animals showed scat-

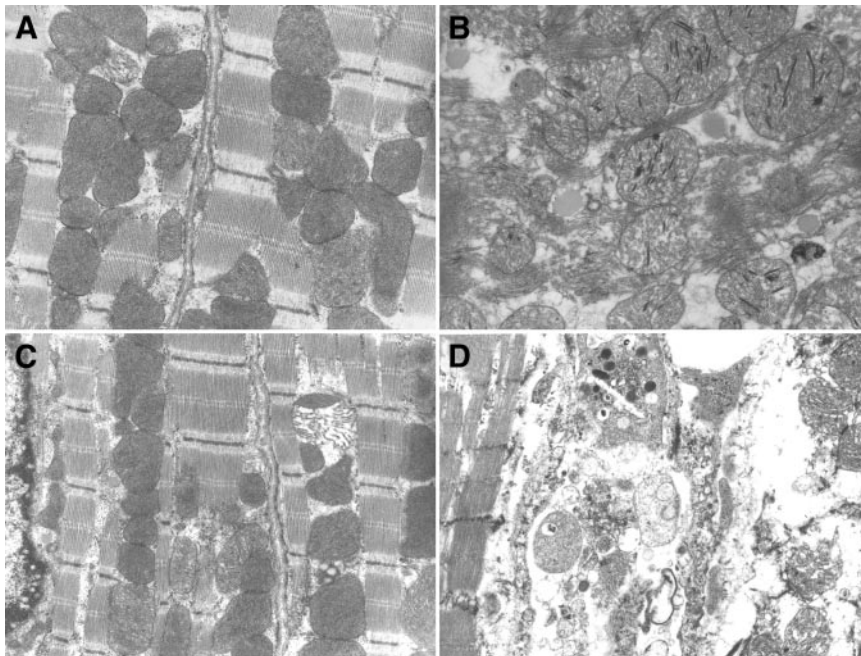


**FIGURE 7.** Myocardial TEM photomicrographs ( $\times 27,262$ ) in rat hearts treated by IR30 and IR90 protocols. (A and C) Electron micrographs taken from left ventricular septum of IR30 heart and IR90 heart, respectively. Cytoarchitecture is normal in appearance. (B and D) Electron micrographs taken from LCA ischemic-reperfused area of IR30 heart and IR90 heart, respectively. Most myofibers show a reduced number of contractile elements, breaking of sarcolemma, sarcoplasmic dilution, abnormal nucleus, and hyperplasia of mitochondria. Sparse cristae, lucent matrix, and intramitochondrial dense granules are common in swollen and fragmented mitochondria. IR90 heart exhibited evidence of more severe and irreversible injury.

tered TTC-negative staining in the IAR. Electron microscope analysis demonstrated focal irreversible myocyte injury characterized by flocculent densities within mitochondria from the risk region with  $^{99m}\text{Tc}$ -GLA scan-positive and TTC-positive staining.  $^{99m}\text{Tc}$ -GLA was sensitive enough to be able to detect early mild scattered myocardial infarcts and micronecroses. Obviously, TTC staining might not delineate myocyte injury in detail and neglect micronecroses. Thus, we assessed regional myocardial injury in the ischemic-reperfused rat heart models using both TTC staining and TEM analysis.

Beanlands et al. used a 15-min global ischemia with a complete reperfusion rat heart model in comparison with 90-min ischemia (14). Significantly higher myocardial retention of  $^{99m}\text{Tc}$ -GLA was found in the 90-min ischemia model but not in the 15-min ischemia model. Effluent creatine kinase (CK) measurement demonstrated that 90 min of flow interruption was sufficient to induce myocardial necrosis, whereas 15 min was not. It was reported that the TTC-negative area might contain approximately 13% reversible injury in an LCA occlusion rat model with 20-min ischemia (16). After 20 min of ischemia, myocardial infarct is markedly increased and further exacerbated by reperfusion. With 30 min of coronary occlusion, the necrotic area can be clearly delineated within the myocardium with the TTC staining technique. Therefore, to investigate in vivo kinetic properties of  $^{99m}\text{Tc}$ -GLA for assessing the severity of myocardial ischemia-reperfusion injury, we selected rat heart models with 30- and 90-min LCA occlusion followed by reperfusion and compared the severities of irreversible necrosis. As a result, the radioactivities and sizes of  $^{99m}\text{Tc}$ -GLA hot spots were significantly distinguishable between the hearts subjected to different durations of ischemia. The high avidity of  $^{99m}\text{Tc}$ -GLA for the infarct makes its uptake visualizable within 10 min after intravenous administration. Forty-five minutes after injection, the ratios of hot spots to normal zone radioactivities showed a significant difference between the 30- and 90-min ischemia heart models.

Few previous studies specifically determined myocardial washout kinetics of  $^{99m}\text{Tc}$ -GLA in vivo. The results of our study show that 30 min of LCA occlusion followed by a 30-min reperfusion induces a significantly slower washout of  $^{99m}\text{Tc}$ -GLA in the necrotic myocardium compared with that of the normal myocardial zone. The kinetic alteration of  $^{99m}\text{Tc}$ -GLA is markedly accelerated by 90-min LCA occlusion. A biexponential function was found to be the best fit for describing the washout pattern of  $^{99m}\text{Tc}$ -GLA. A rapid early clearance phase followed by a slow second phase was observed in the ischemic-reperfused myocardium and normal zone. In the early phase, which mainly reflects blood perfusion and effusion, the  $t_{1/2}$  of  $^{99m}\text{Tc}$ -GLA from the biexponential function did not differ between the infarct and normal zones. In the second phase, which reflects cellular efflux of  $^{99m}\text{Tc}$ -GLA, the  $t_{1/2}$  of the hot spot was significantly longer than that in the normal myocardium. The principal differences among the hearts subjected to 30- and

90-min ischemia resulted from a differential late phase washout. The longer  $t_{1/2}$  or slow clearance in the second phase was more pronounced in 90-min ischemic hearts. These data indicate that the severity of myocardial injury induced by different durations of ischemia with reperfusion in rat heart models can be quantitatively analyzed with  $^{99m}\text{Tc}$ -GLA dynamic imaging using the fast acquisition capability of FASTSPECT.

Using FASTSPECT imaging, our previous study has demonstrated that the infarct size can be quantitatively measured in rat heart models with  $^{99m}\text{Tc}$ -sestamibi defects (9).  $^{99m}\text{Tc}$ -Sestamibi myocardial activity correlates the amount of viable myocardium stained by TTC. The extent of the left ventricular perfusion defect on  $^{99m}\text{Tc}$ -sestamibi images reflects the size of the myocardial infarction.  $^{99m}\text{Tc}$ -GLA is accumulated by infarcted tissue only. The results of the present study indicate that hot spot imaging with  $^{99m}\text{Tc}$ -GLA is promising for the determination of infarct size in persistently occluded or reperfused myocardial infarcts. Measurement of FASTSPECT imaging demonstrated that the hot spot size of  $^{99m}\text{Tc}$ -GLA correlates well with the infarct size determined by TTC staining. In comparison with  $^{99m}\text{Tc}$ -sestamibi imaging, in which the defects are clearly contrasted with normal myocardium, negative accumulation of  $^{99m}\text{Tc}$ -GLA in normal myocardium makes the quantitative analysis difficult to calculate the percentage of infarct over the whole left ventricle in the heart with a small-size infarct. We used the early blood-pool image to identify the left ventricular wall range so that the percentage of infarct size could be quantified in the present study. Using a computed 3D display, absolute infarct volume may be measured more reliably, which provides insight into prognosis after acute myocardial infarction.

To our knowledge, the in vivo kinetics of cardiovascular radiopharmaceuticals have not been investigated previously with dynamic high-resolution SPECT imaging in rat heart models. Large animals, such as canines, are often used for in vivo experimental imaging in coronary artery disease. However, the cost for large animals is high, and experience with surgical techniques is required. The small-animal heart model, such as rodents, offers advantages over large-animal models, such as low cost, simple procedures in surgery, and a high successful rate in modeling. In addition, many gene therapy strategies for the treatment of cardiac failure and long-term myocardial protection are being studied in rodent models with noninvasive imaging requirement. In recent years, high-resolution tomographic imaging systems have become available for small-animal studies in basic biomedical science so that many experimental procedures in large-animal cardiac models can be performed in rat models (17). In our rat heart models of the present study, dynamic cardiac images were acquired with FASTSPECT using procedures similar to those required by clinical physicians. But tomographic dynamic imaging cannot be achieved by a regular clinical rotating SPECT camera. With the advantages of FASTSPECT, the myocardial radioactivity in the present study could be quantified accurately and the washout kinet-

ics of  $^{99m}\text{Tc}$ -GLA were determined effectively. The quantitative analysis of myocardial infarct on tomographic images showed a significant correlation with biochemical staining measurement.

## CONCLUSION

The results of this study demonstrate the property of  $^{99m}\text{Tc}$ -GLA to positively identify acute infarct myocardium.  $^{99m}\text{Tc}$ -GLA can mark nonviable regions by hot spot imaging in myocardium with infarct. Therefore, the severity of myocardial injury induced by different durations of ischemia after reperfusion could be assessed noninvasively and quantitatively. This agent would appear to be clinically useful to determine the location and size of acute infarcted myocardium very early.  $^{99m}\text{Tc}$ -GLA imaging may not only provide an imaging tool to diagnose equivocal myocardial infarct in patients with heart attacks, allowing differentiation of acute from recent infarcts, but also direct the use of thrombolytic therapy. Quantitative analyses on dynamic images with  $^{99m}\text{Tc}$ -GLA would make it possible to identify myocardial acute necrosis earlier and more accurately and provide a unique, noninvasive tool for evaluation of patient prognosis. The FASTSPECT imaging with the ischemic-reperfused rat heart model provides a solution-specific approach with high spatial resolution and fast dynamic acquisition for kinetic studies of new myocardial imaging agents as the evidence of its major role in the present study.

## ACKNOWLEDGMENTS

The authors acknowledge Peggy McCuskey and Gina Zhang for their expertise in preparing tissues for electron microscopy. This work was supported by National Institutes of Health grants P41 EB002035 and R24 CA83148.

## REFERENCES

1. Orlandi C, Crane PD, Edwards S, et al. Early scintigraphic detection of experimental myocardial infarction in dogs with  $^{99m}\text{Tc}$  glucuric acid. *J Nucl Med.* 1991;32:263–268.
2. Khaw BA, Nakazawa A, O'Donnell SM, Pak KY, Narula J. Avidity of technetium  $^{99m}$  glucurate for the necrotic myocardium: in vivo and in vitro assessment. *J Nucl Cardiol.* 1997;4:283–290.
3. Narula J, Petrov A, Pak KY, Lister BC, Khaw BA. Very early noninvasive detection of acute experimental nonreperfused myocardial infarction with  $^{99m}\text{Tc}$ -labeled glucurate. *Circulation.* 1997;95:1577–1584.
4. Mariani G, Villa G, Rossettin PF, et al. Detection of acute myocardial infarction by  $^{99m}\text{Tc}$ -labeled D-glucuric acid imaging in patients with acute chest pain. *J Nucl Med.* 1999;40:1832–1839.
5. Arteaga de Murphy C, Ferro-Flores G, Villanueva-Sanchez O, et al.  $^{99m}\text{Tc}$ -Glucurate for detection of isoproterenol-induced myocardial infarction in rats. *Int J Pharm.* 2002;233:29–34.
6. Khaw BA, Silva JD, Petrov A, Hartner W. Indium-111 antimyosin and Tc- $^{99m}$  glucuric acid for noninvasive identification of oncotic and apoptotic myocardial necrosis. *J Nucl Cardiol.* 2002;9:471–481.
7. Kaufman N, Gavan TL, Hill RW. Experimental myocardial infarction in the rat. *Arch Pathol.* 1959;67:482–488.
8. Deloche A, Fabiani JN, Camilleri JP, et al. The effect of coronary artery reperfusion on the extent of myocardial infarction. *Am Heart J.* 1977;93:358–366.
9. Liu Z, Kastis GA, Stevenson G, et al. Quantitative analysis of acute myocardial infarction in rat hearts with ischemia-reperfusion using a high-resolution stationary SPECT system. *J Nucl Med.* 2002;43:933–939.
10. Klein WP, Barrett HH, Pang IW, et al. FASTSPECT: electrical and mechanical design of a high-resolution dynamic SPECT imager. In: *Conference Record of the 1995 IEEE Nuclear Science Symposium and Medical Imaging, San Francisco, California.* Vol. 2. Los Alamitos, CA: Institute of Electrical and Electronics Engineers, Inc.; 1995:931–933.
11. Kastis GK, Barber HB, Barrett HH, et al. High resolution SPECT imager for three-dimensional imaging of small animals [abstract]. *J Nucl Med.* 1998; 39(suppl):9P.
12. Rowe RK, Aarsvold JN, Barrett HH, et al. A stationary hemispherical SPECT imager for three-dimensional brain imaging. *J Nucl Med.* 1993;34:474–480.
13. National Research Council. *Guide for the Care and Use of Laboratory Animals.* NIH Publication 85-23. Bethesda, MD: U.S. Department of Health and Human Services, National Institutes of Health; 1985.
14. Beanlands RS, Ruddy TD, Bielawski L, Johansen H. Differentiation of myocardial ischemia and necrosis by technetium  $^{99m}$  glucuric acid kinetics. *J Nucl Cardiol.* 1997;4:274–282.
15. Johnson LL, Schofield L, Mastrofrancesco P, Donahay T, Farb A, Khaw BA. Technetium- $^{99m}$  glucurate uptake in a swine model of limited flow plus increased demand. *J Nucl Cardiol.* 2000;7:590–598.
16. Takashi E, Ashraf M. Pathologic assessment of myocardial cell necrosis and apoptosis after ischemia and reperfusion with molecular and morphological markers. *J Mol Cell Cardiol.* 2000;32:209–224.
17. Weber DA, Ivanovic M. Ultra-high-resolution imaging of small animals: implications for preclinical and research studies. *J Nucl Cardiol.* 1999;6:332–344.